STRUCTURE AND CONDUCTIVITY OF CALCIA STABILIZED ZIRCONIA CERAMICS, MANUFACTURED FROM FREEZE-DRIED NANOPOWDER

O.Yu. Kurapova[1,2], O.V. Glumov[1], M.M. Pivovarov[2], S.N. Golubev[2] and V.G. Konakov[1,2]

[1]St. Petersburg State University, Universitetskaya emb. 7/9, St. Petersburg, 199034, Russia
[2]Glass and Ceramics Ltd., 9 Linia V.O., 20, St. Petersburg, 199004, Russia

Abstract. The work reports the investigation of the structure and electrical conductivity of xCaO-$(100-x)$ZrO$_2$ (x=9, 12, and 15 mol.%) ceramics. Calcia stabilized zirconia ceramics was manufactured from freeze-dried nanopowder by annealing of compacted samples at 1823K for 3 hours. Structure and composition of samples were investigated by SEM, EDX, and XRD analysis. Electrical properties of ceramics were investigated via impedance spectroscopy technique in the range 556-1033K. It was shown that the conductivity of xCaO-$(100-x)$ZrO$_2$ (x=9 and 12 mol.%) ceramics is ~10^{-2} S/cm at 1000K. Temperature dependencies of grain and grain boundary conductivity were obtained for all ceramic compositions. The values of activation energies of conductivity and blocking coefficients showed that grain boundaries in ceramics are thin and discontinuous. The mechanism of conductivity in CaO-ZrO$_2$ system was suggested

1. INTRODUCTION

Among other zirconia based materials, solid electrolytes with ionic conductivity are important group of materials for high temperature applications [1-3]. Cubic zirconia solid solutions, stabilized by CaO [4], MgO [5], Y$_2$O$_3$ [6] and some other rare earth oxides, are the most known. Unipolar ionic character of conductivity of such solid solutions at high temperatures allows to use them as solid electrolytes (SE) in certain galvanic cells i.e. oxygen pumps [7,8] or oxygen sensors in combustion cameras, energy apparatus, ferrous and non-ferrous metallurgy, glass-making production, refractoriness etc for precise in situ control of the oxygen partial pressure [2,9,10].

The conductivity of zirconia based solid electrolytes (SE) significantly depends on solid solution structure, type and concentration of the stabilizing dopant, as well as the operating temperature [11]. Despite that broad cubic solid solution region is formed in many binary systems, Y$_2$O$_3$ – ZrO$_2$ (YSZ) system only is used for practical applications. As notable ionic conductivity in such SE takes place at higher ~673K [1], the scientists all over the globe continue the search towards new ceramic compositions, allowing the decrease of the working temperature and sensitivity limit of zirconia SE. A number of ternary systems were suggested as an alternative to YSZ system as, e.g. ZrO$_2$-HfO$_2$-Y$_2$O$_3$ [12,13], Ce$_2$O$_3$-Y$_2$O$_3$-ZrO$_2$ [14, 15] or ZrO$_2$-TiO$_2$-Y$_2$O$_3$ [16]. Promising thermodynamic data on the evaporation of binary Lu$_2$O$_3$-ZrO$_2$ and La$_2$O$_3$ –ZrO$_2$ systems was obtained in [17, 18], showing their excellent stability and performance at very high temperatures (~2100K). However the application of such systems is still limited by low availability (high price) rare-

earth oxides. Since 1970th calcia stabilized zirconia (CSZ) gains the attention of the researchers due to its relatively high conductivity and availability of starting materials [19]. That is why it is, most probably, one of the most studied. Thermochemical properties [20], phase relations in this system [4,21], temperature dependence of ionic conductivity [20,22] are well known. However CaO is significantly volatile at high temperatures, which limits the stability of calcia based zirconia solid solutions [1,20]. Plenty of literature data allows to use CSZ ceramics as a great model system.

It is mentioned in [23], the precise control of ceramics microstructure is regarded to be a key for ionic conductivity increase. In this way the use of nanosized precursor powders is preferable for ceramic SE manufacturing. In the recent works of authors [24,25] it was shown that the combination of sol-gel synthesis and freeze drying results in nanosized powders with required dispersity and structure. Their intermediate treatment, compacting at certain optimized conditions and then thermal treatment at 1773-1973K result in SE with refined microstructure. Latter could give rise for high ionic conductivity of the investigated system. Impedance spectroscopy is considered as one of the most effective approaches to study such electrochemical processes. This technique makes possible the separation of the inputs of different structural components of ceramics in the integral conductivity of polycrystalline ceramics [13]. As a result the effect of microstructure (i.e. the synthesis technique), possible phase transitions and some other phenomena on the ionic conductivity of ceramics can be studied in details. Thus the aim of the present work was to study the effect of structure on the electrochemical properties of xCaO-(100-x)ZrO$_2$ (x = 9, 12, 15 mol.%) ceramics.

2. EXPERIMENTAL

2.1. Ceramics synthesis

Nanosized xCaO-(100-x)ZrO$_2$ (x = 9, 12, 15 mol.%) precursor powders were obtained by reversed co-precipitation from diluted aqueous salt solution and freeze drying according to the technique, described in [25]. Powders were annealed at 923K for 3 hours in air. Thermal treatment temperature was chosen according to simultaneous thermal analysis (STA) data [25]. The obtained powders were milled in a planetary mill (Pulverisette 6, Fritzch, 400 rpm, 1 hour) and then compacted into the pellets (diameter 10.5 mm, height 6 mm) at pressure 3.5 ton/sm^2. The pellets of 12CaO-88ZrO$_2$ and 15CaO-

85ZrO$_2$ (mol.%) underwent intermediate annealing step to prevent recrystallization of ceramics. These pellets were crushed, milled once again and compacted into the pellets of the same size. Then all ceramic compositions were finally annealed at 1823K for 3 hours.

2.2. Analysis

Simultaneous thermal analysis (STA, STA 449 F1 Jupiter Netzsch, nitrogen ambience, the heating velocity 10 deg./min.) was performed in order to investigate phase transition temperature in precursors after synthesis. Microstructure of ceramics was investigated by scanning electron microscopy (SEM, Hitachi S-3400N, accelerating voltage 20 kV with the equipment for energy dispersive spectroscopy EDX analysis, unit AzTec Energy 350). Phase composition of ceramics was identified using X-ray diffraction analysis (XRD, Shimadzu XRD-6000, Cu-Kα radiation, λ = 1.54 Å, room temperature). Powder diffraction data was used for phase composition identification [26].The mean size of crystallites was estimated via Scherrer's equation using the profile of the peak at 2θ=29.5°. Electrochemical impedance (Autolab PGSTAT 302N Potentiosytat/Galvanostat) was used to investigate the electrochemical properties of calcia stabilized zirconia ceramics. Electrochemical impedance was measured in the temperature range from 556 to 1033K. Experiments were performed in the quartz cell with Pt electrodes and contacts.

3. RESULTS AND DISCUSSION

The microphotos of the unpolished surface of CaO-ZrO$_2$ ceramics at different magnification are shown in Fig. 1.

As it is seen from the Figure, ceramics with different CaO content are well formed. 9CaO-91ZrO$_2$ (9CSZ) and 12CaO-88ZrO$_2$ (12CSZ) samples (see Figs. 1a and 1b) consist of micron-sized grains, separated by well defined grain boundaries with residual open porosity. Grain size of both samples is close to each other and varies from 2 to 20 μm. The grain boundaries are straight. The angles between grains are close to 90°, indirectly indicating the cubic structure of ceramics (Fig. 1d). The microstructure of 15CaO-85ZrO$_2$ (15CSZ) ceramics differs from 9CSZ and 12CSZ samples. From Fig. 1c it is seen that amorphous zones are present in ceramics. Grain size estimated from SEM is 2-10 μm. Small grains with size less than 4-5 μm prevail in structure of sample. It is possibly due to recrystallization, that took place during the annealing. Chemical com-
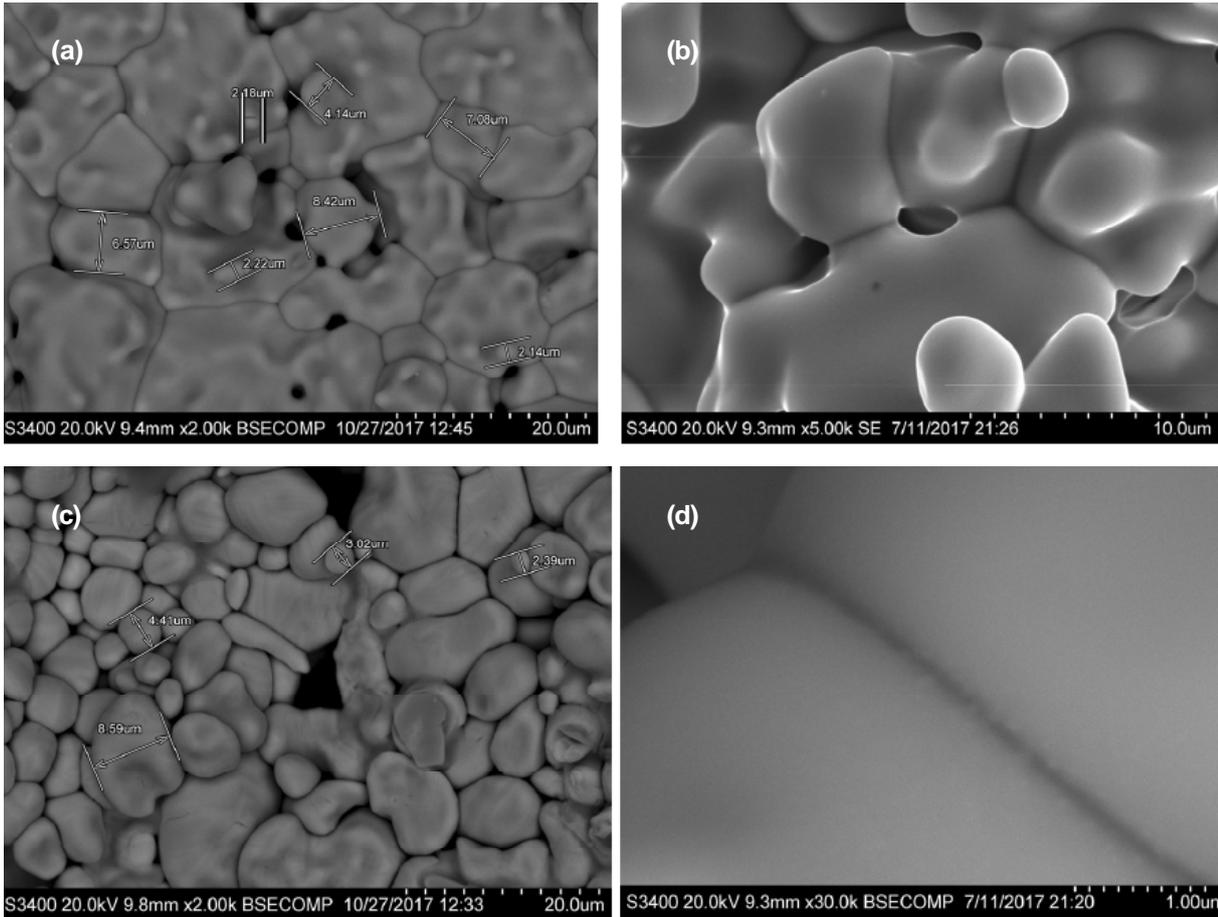
Fig. 1. SEM microphotographs of xCaO-(100-x)ZrO$_2$ ceramics surface manufactured from nanopowder (a) x=9 mol.%, magnification x2 000; (b) x=12 mol.%, magnification x5 000; (c) x=15 mol.%, magnification x2 000; (d) grain boundary of 12CaO-88ZrO$_2$ ceramics, magnification x30 000.

position of ceramics was estimated via EDX data. The final composition recalculated from EDX spectra is presented in Table 1 together with brutto composition.
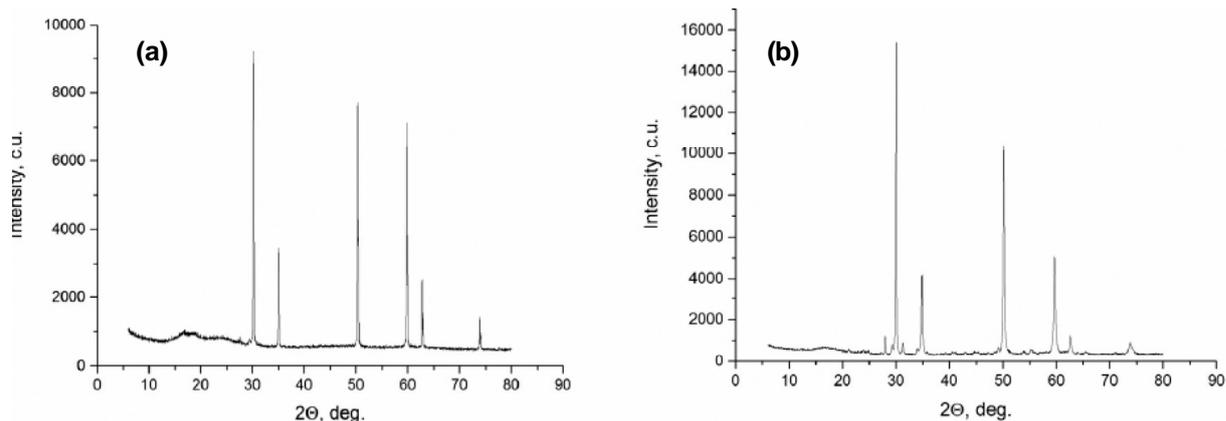
Despite calcia is rather volatile at temperatures higher 1773K, the composition of ceramics after the annealing at 1823K for 3 hours nearly corresponds to the composition given upon the synthesis. Small amount of HfO$_2$ is present in all samples. Hafnia is isomorphous to zirconia and usually present in the starting materials. At the same time it acts as an additional stabilizer of cubic solution [12]. No other admixtures were detected in all ceramic samples,

i.e. no impurities were introduced during nanopowder synthesis and milling in a planetary mill. So one can expect the grain boundaries in ceramics to be free of segregations. XRD patterns of 9CSZ and 15CSZ ceramics are presented in Fig. 2.

From Fig. 2a one can see that 9CaO-91ZrO$_2$ ceramics is a single phase. All peaks in XRD pattern correspond to cubic zirconia solid solution (i.e. 2θ=29.5, 35, 51, 58°, etc). The same result was obtained for 12CaO-88ZrO$_2$ ceramics. The difference between compositions containing 9 and 12 mol.% of calcia is only in the peaks intensity. The increase of CaO content results in ceramics having mono-

Table 1. Brutto composition and final composition estimated by EDX data.

Composition upon synthesis (brutto), mol.%		Final composition, mol.%		
CaO	ZrO$_2$	CaO	ZrO$_2$	HfO$_2$
9	91	8.6	90.3	1.1
12	88	11.3	87.6	1.1
15	85	14.1	84.6	1.3

Fig. 2. XRD patterns of (a) $9CaO-91ZrO_2$ ceramics; (b) $15CaO-85ZrO_2$ ceramics.

clinic phase admixture to cubic solid solution. The estimated amount of monoclinic zirconia is 5-7%. The presence of second phase confirms the suggestion on ceramics recrystallization. Lattice parameters along with crystallinity degree and crystallite size estimated from XRD data are listed in Table 2.

As it is seen from the Table crystallinity degree of all samples lies in range 87-98%. Note, that crystallinity degree slightly decreases with the increase of CaO content. Lower value of crystallinity of $15CaO-85ZrO_2$ is, most probably due to recrystallization. In all cases crystallites are nanosized, i.e. for all ceramic compositions investigated cubic solid solution is well-formed. From SEM, EDX, and XRD data one can see that the cryothemical approach coupled with milling in a planetary mill is an effective way to obtain ceramics of given composition free of impurities characterized by required microstructure and phase composition. It allows to suggest the sufficient conductivity level in case of 9CSZ and 12CSZ ceramic solid electrolytes. Decreased ionic conductivity can be expected for $15CaO-85ZrO_2$ ceramics. Impedance spectra were obtained for $xCaO-(100-x)ZrO_2$ ceramics ($x = 9$, 12 and 15 mol.%) in the range 556-1033K.
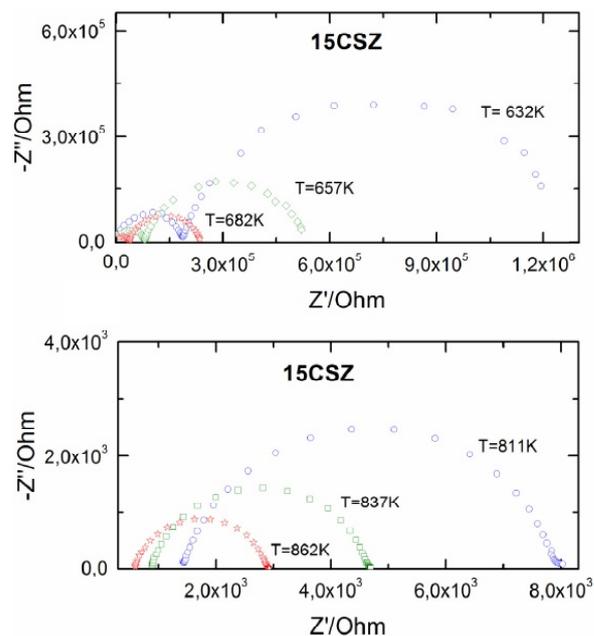

Fig.3. Impedance spectra of $15CaO-85ZrO_2$ ceramics taken (a) at high and (b) low frequency.

Typical spectra obtained for $15CaO-85ZrO_2$ ceramics taken at high and low frequency are presented in Fig. 3.

As it is seen from Fig. 3a two distinguished semicircles corresponding to ionic conductivity are

Table 2. Crystallinity, crystallite size and phase composition data estimated from XRD patterns.

| Composition, mol.%	Phase composition	Crystallinity, %	Crystallites size, nm estimated by Sherrer's equation	Lattice parameter, Å
$9CaO-91ZrO_2$	Cubic solid solution	98	54	5.128
$12CaO-88ZrO_2$	Cubic solid solution	95	60	5.126
$15CaO-85ZrO_2$	Cubic solid solution + monoclinic zirconia	87	26	5.135
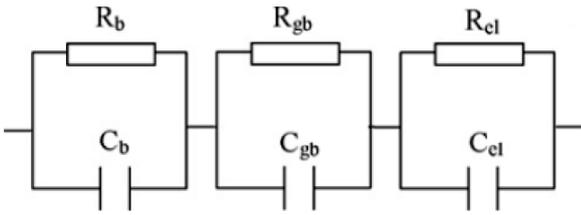
Fig. 4. Equivalent circuit for zirconia based solid solutions.

present at 657K in the impedance spectrum of 15CSZ ceramics. Only one semi-circle can be seen in spectra taken at higher temperatures which can be referred to grain conductivity according to the equivalent circuit, presented in Fig. 4. Let us note that spectra, taken at ~1000K are not presented in the work. In the low-frequency area at higher 1000K the diffusion of Pt electrodes in the bulk of ceramic membrane takes place. Thus electronic conductivity is observed at high temperatures, see e.g. [12]. Similar impedance data were obtained for 9CaO-91ZrO$_2$ and 12CaO-88ZrO$_2$ ceramics. Since for all compositions investigated both semi-circles in impedance spectra (i.e. in low and high frequency regions) are well defined, grain and grain boundary

inputs into the integral ceramics conductivity of polycrystalline ceramics were distinguished.

Temperature dependences of grain and grain boundary conductivities of CaO-ZrO$_2$ system are shown in Fig. 5.

As it is seen from Fig. 5 linear dependencies of both bulk and grain boundary conductivities are observed for all ceramic composition in the range 556-1000K. Conductivity is ionic with no admixture of the electronic component. The conductivity values of SE containing 9 and 12 mol.% of CaO are rather close to 10^{-2} S/cm at 1000K. That is, likely, due to similar SE structure. The suggestion is in accordance with SEM and XRD data (see Figs. 1 and 2). As it was expected, because of monoclinic ZrO$_2$ admixture, the conductivity of 15CSZ solid electrolyte is about 1.5 order of magnitude lower (see Fig. 2b). According to [1], the presence of monoclinic zirconia and CaZrO$_3$ is typical for calcia stabilized zirconia ceramics with high CaO content and significantly decreases the integral ionic conductivity. Let us note that the conductivity values obtained in the present work are close to the data of [27] for CSZ ceramics obtained by rapid combustion route
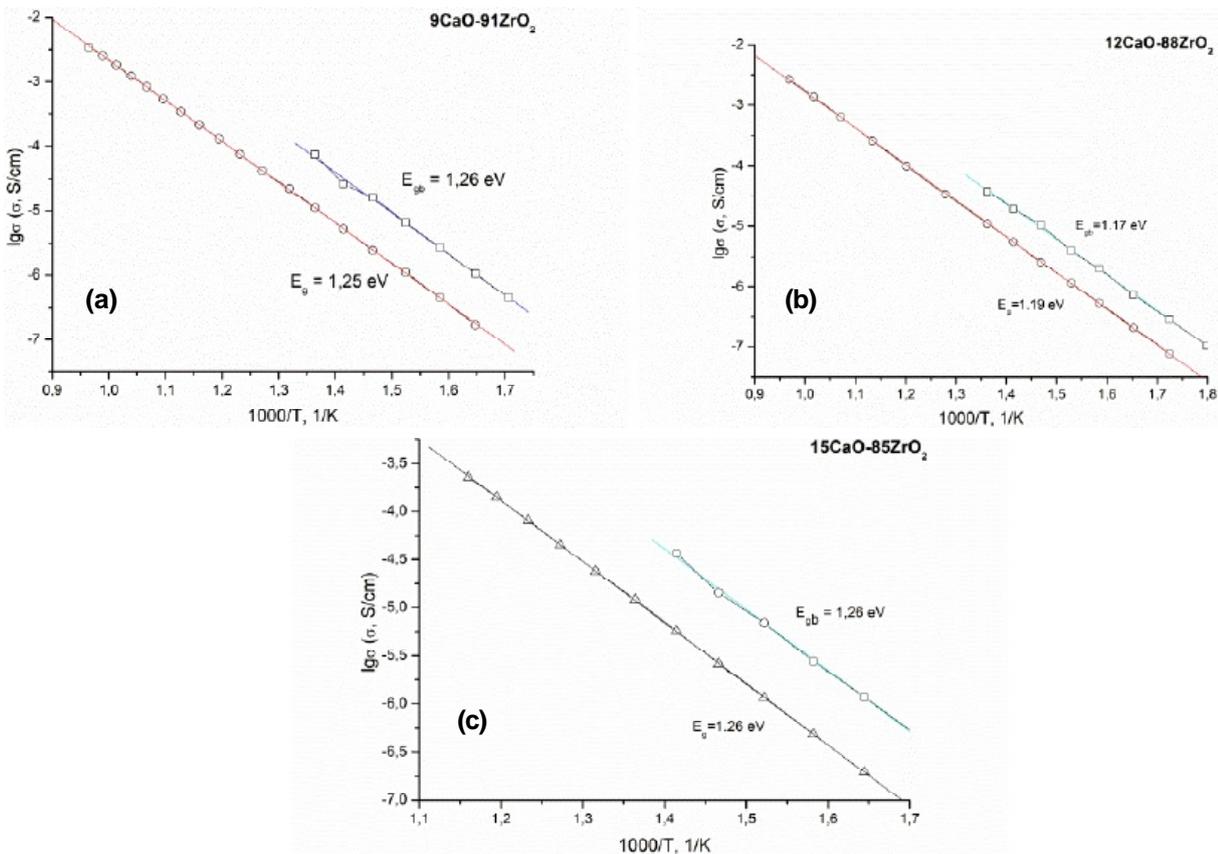
Fig.5. Temperature dependences of grain and grain boundary conductivities of (a) 9CaO-91ZrO$_2$; (b) 12CaO-88ZrO$_2$; (c) 15CaO-85ZrO$_2$ solid electrolytes.

Table 3. Activation energy of conductivity (Ea) of different structure components of ceramics.

| | Activation energy – Ea, eV | | |
	$9CaO\text{-}91ZrO_2$	$12CaO\text{-}88ZrO_2$	$15CaO\text{-}85ZrO_2$
grain	1.25	1.19	1.26
grain boundaries	1.26	1.17	1.26
Blocking coefficient, β	0.165	0.22	0.14

and conductivity of ZrO_2-HfO_2-Y_2O_3 solid electrolytes obtained by reversed co-precipitation [12].

For all compositions investigated, the values of grain boundary conductivity are half to one order of magnitude lower than the ones for the grain conductivity. As it usually comes for zirconia based SE, grain boundary conductivity is at least two orders of magnitude lower then grain conductivity [13]. That allows to suggest, that the grain boundaries are discontinuous. In order to check this hypothesis for polycrystalline calcia stabilized zirconia ceramics, the activation energy of conductivity was calculated using Arrhenius equation, Eq. (1):

$$\sigma = \sigma_0 \exp\left(\frac{E_\alpha}{RT}\right), \tag{1}$$

where T – absolute temperature, R – universal gas constant, σ_0 – pre-exponential factor. The obtained values are presented in Table 3.

As it is seen from Table 3, activation energy of conductivity for $9CaO\text{-}91ZrO_2$ and $15CaO\text{-}85ZrO_2$ ceramics is 1.26 eV, which is in good accordance with literature for $CaO\text{-}ZrO_2$ system, i.e. ~1.3 eV [27]. In case of $12CaO\text{-}88ZrO_2$ the value of activation energy is lower. It can be due to refined microstructure in the bulk of sample. Let us note that the grain and grain boundaries activation energies of

conductivity are close to each other for all the samples. That confirms the idea about grain boundaries being discontinuous. As in this case the calculation of grain boundary thickness is not possible, blocking coefficient β (i.e. the fraction of grain boundary resistivity in the integrate resistivity) was calculated:

$$\beta = \rho_{gb} / \left(\rho_g + \rho_{gb}\right), \tag{2}$$

where ρ_g, ρ_{gb} – specific resistivity of grains and grain boundaries, respectively. The values obtained are listed in Table 3 together with activation energy of conductivity. For all ceramic compositions β lies in the range 0.14-0.22, i.e. grain boundaries of all ceramic compositions are rather thin and free of admixture segregations. Local maximum of the blocking coefficient is observed in case of $12CaO\text{-}88ZrO_2$ composition. A bit thicker grain boundaries are, likely, due to well-formed microstructure with low porosity either on surface and in the bulk of ceramic samples as well as defined and straight grain boundaries. That allows to suggest the existence of simplified ways of both ion carriers migration and blocking ways. It could explain similar temperature dependencies of conductivity obtained for $12CaO\text{-}88ZrO_2$ and $9CaO\text{-}91ZrO_2$ ceramics. The comparison of grain and grain boundary conductivities of
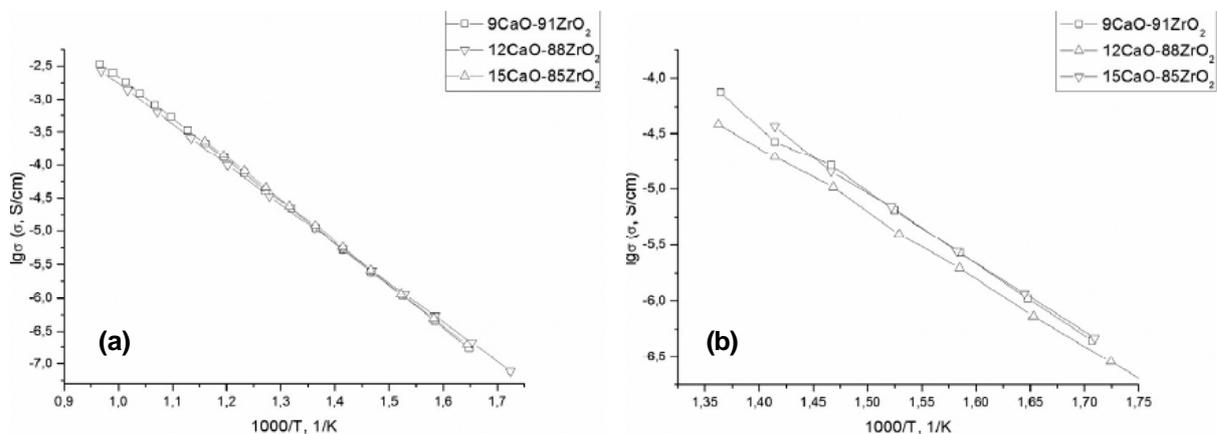
Fig.6. Temperature dependencies of (a) grain conductivity; (b) grain boundary conductivity for zirconia based ceramics with different CaO content.

ceramics with different calcia content are shown in Fig. 6.

As it is seen from Fig. 6a, the temperature dependencies of grain conductivity are very close for all investigated compositions. The picture observed is, likely, due to similar grain size of ceramics with different calcia content and is in accordance with SEM data (see Fig. 1). So the cryochemical technique used for ceramic manufacturing is scalable for different ceramic compositions. Similar results were obtained upon comparison of temperature dependence of grain boundaries conductivity (see Fig. 6b). The only difference is that grain boundary conductivity of $12CaO-88ZrO_2$ ceramics is a bit lower than the values for $9CaO-91ZrO_2$ and $15CaO-85ZrO_2$ compositions in all temperature range. It is, most likely, due to a bit higher value of blocking coefficient i.e. thicker grain boundaries. Summarizing the data on the conductivity of structural components, activation energy of conductivity and blocking coefficient one can conclude that at low temperatures the conductivity in $CaO-ZrO_2$ is realized mostly on the SE surface. Up on temperature increase up to ~780K ion carriers move in the grains (SE bulk).

4. CONCLUSIONS

Via SEM, EDX, XRD, and impedance spectroscopy it was shown that cryochemical approach is an effective and scalable way to manufacture ceramics based on cubic zirconia solution having high conductivity values. Ceramics with different CaO content consists of microsized grains divided by rather thin discontinuous grain boundaries free of segregations. Linear dependence of both bulk and grain boundary conductivities was obtained for xCaO-$(100-x)$ZrO$_2$ ($x = 9, 12, 15$ mol.%) ceramics in the range 556-1000 K. Sufficient ionic conductivity of $9CaO-91ZrO_2$ and $12CaO-88ZrO_2$ ceramics at ~1000K allows to recommend them as solid electrolytes for oxygen sensors fabrication.

ACKNOWLEDGEMENTS

REFERENCES

[1] R. Stevens, *Zirconia and zirconia ceramics* (Magnesium Electron, Twickenham, UK, 1986).

[2] S. Akbar, P. Dutta and Ch. Lee // *International journal of applied ceramic technology* **4** (2006) 302.

[3] J. W. Fergus // *Journal of Power Sources* **162** (2006) 30.

[4] V.S. Stubican and P.S. Ray // *J. Amer. Ceram. Soc.* **60** (1977) 534.

[5] C. F. Grain // *J. Amer. Ceram. Soc.* **50** (1967) 288.

[6] V. S. Stubican, R. C. Hink and S.P. Ray // *J. Amer. Ceram. Soc.* **61** (1978) 17.

[7] A. Q. Pham and R. S. Glass // *Electrochimica acta* **43** (1998) 2699.

[8] D. Yuan and F.A. Kröger // *Journal of The Electrochemical Society* **116** (1969) 594.

[9] H. J. Neef // *Energy* **34** (2009) 327.

[10] V. G. Konakov // *Journal of Solid State Electrochemistry* **15** (2011) 77.

[11] B. C. H. Steele // *Materials Science and Engineering B* **13.2** (1992) 79.

[12] N. N. Novik, O. V. Glumov, S. N. Golubev, V. G. Konakov and I. Yu. Archakov // *Rev. Adv. Mater. Sci.* **43** (2015) 67.

[13] *Impedance Spectroscopy: Theory, Experiment and Application*, ed. by E. Barsoukov and J.R. Macdonald (Willey, 2005).

[14] V.G. Konakov, S. Seal, E.N., Solovieva, D.A. Ivanov-Pavlov, M.M. Pivovarov, S.N. Golubev and A.V. Shorohov // *Rev. Adv. Mater. Sci.* **16** (2007) 96.

[15] J.-D. Lin and J.-G. Duh // *J. Amer. Ceram. Soc.* **80** (1997) 92.

[16] H. Naito and H. Arashi // *Solid State Ionics* **53** (1992) 436.

[17] S. I. Lopatin and S. M. Shugurov // *J. Chem. Thermodynamics* **72** (2014) 85.

[18] S. M. Shugurov, O. Y. Kurapova, S. I. Lopatin, V. G. Konakov and E. A. Vasil'eva // *Rapid Communications in Mass Spectrometry* **31** (2017) 2021.

[19] N. M. Beekmans and L. Heyne // *Electrochimica Acta* **21** (1976) 303.

[20] N.S. Jacobson, *Thermodynamic properties of some metal oxide-zirconia systems* (National aeronautics and space administration, Cleveland, OH, Lewis research center, 1989, ą. NASA-E-5060).

[21] K. Wang, Ch. H Li and Y. H. Gao. // *J. Amer. Ceram. Soc.* **92** (2009) 1098.

[22] S.H. Chu and M. A. Seitz // *Journal of Solid State Chemistry* **23** (1978) 297.

[23] A. Kocjan, V. Pouchly and Z. Shen // *Journal of the European Ceramic Society* **35** (2015) 1285.

[24] V. G. Konakov, O. Y. Kurapova, N. V. Borisova, S. N. Golubev, V. M. Ushakov, E. V. Koroleva and I. Y. Archakov // *Journal of Sol-Gel Science and Technology* **82** (2017) 214.

[25] O. Yu. Kurapova, D. V. Nechaeva, A. V. Ivanov, S. N. Golubev, V. M. Ushakov and V. G. Konakov // *Rev. Adv. Mater. Sci.* **47** (2016) 96.

[26] *PDF (powder diffraction file) database*, release 2, 2012.

[27] A. K. Shukla // *Materials Science and Engineering: B* **40** (1996) 153.